Acta Biochim Biophys Sin, 2017, 49(4), 355–360
doi: 10.1093/abbs/gmx015
Advance Access Publication Date: 10 March 2017
Short Communication

Short Communication

The effect of aluminum ion on the aggregation of human islet amyloid polypeptide (11-28)

Lanlan Su[1], Cheng Lu[1], Peng Yan[1], Nan Zhang[1], Sheng Cai[2], Gongjun Zhang[2], Xingfei Zhou[1,*], and Bin Li[3,*]

[1]School of Science, Ningbo University, Ningbo 315211, China, [2]Ningbo Institute of Material Technology and Engineering, Chinese Academy of Sciences, Ningbo 315201, China, and [3]Laboratory of Physical Biology, Shanghai Institute of Applied Physics, Chinese Academy of Sciences, Shanghai 201800, China

*Correspondence address. Tel/Fax: +86-574-87600744; E-mail: zhouxingfei@nbu.edu.cn (X.Z.)/Tel: +86-215-9553998; Fax: +86-215-9552394; E-mail: Libin@sinap.ac.cn (B.L.)

Received 16 December 2016; Editorial Decision 21 January 2017

Abstract

Metal ions play a critical role in human islet amyloid polypeptide (hIAPP) aggregation, which is believed to be closely associated with β-cell death in type II diabetes. In this work, the effect of Al^{3+} on the aggregation of hIAPP (11-28) was studied by several different experimental approaches. Atomic force microscopy measurements showed that Al^{3+} could remarkably inhibit hIAPP(11-28) fibrillogenesis, while Zn^{2+} had a slight promotion effect on peptide aggregation, which was also confirmed by Thioflavin T fluorescence observation. Furthermore, X-ray photoelectron spectroscopy measurement indicated that Al ions might form chemical bonds with neighboring atoms and destroy the secondary structures of the protein. Our studies could deepen the understanding of the role of metal ions in the aggregation of amyloid peptides.

Key words: metal ion, hIAPP peptides, atomic force microscopy, Thioflavin T fluorescence, X-ray photoelectron spectroscopy

Introduction

The misfolding of amyloid peptides is associated with a number of human diseases such as type II diabetes mellitus (T2DM), Alzheimer's disease (AD), and Parkinson's disease (PD) [1–3]. Human islet amyloid peptide (hIAPP, also known as human amylin), a 37-residue peptide cosecreted with insulin by islet β-cells, has the propensity to aggregate and form amyloid fibril deposits even at low micromolar concentrations [4–7]. The aggregation of hIAPP with the characteristic β-sheet secondary structure could lead to the development of islet β-cells dysfunction and death in the pathology of T2D [8–12].

Amyloid aggregation is not only closely related to the amino acid sequence, but also associated with non-genetic factors such as metal ions, pH value, and environmental temperature [13–16]. Particularly, metal ions have been proved to play a significant role in the fibrillization of amyloid peptides [17–22]. For example, Cu^{2+} can interact with hIAPP or Aβ to suppress the fibrosis [23,24]. It has been that Al ion is one of the critical factors in the etiopathogenesis of AD. It could bond to the amide nitrogen and carbonyl oxygen atoms of peptide backbone to form ring structure, seriously destroying the secondary structures of the protein [25]. Amyloid deposition in the brain and pancreas show some striking pathophysiologic similarities, and patients with AD are more likely to develop T2D [26]. Therefore, it is necessary to explore the effect of Al ions on the aggregation of hIAPP and related peptide fragments.

It has been suggested that hIAPP (11-28) fragment is the core structure for the fibrillation of full-length hIAPP [27]. Therefore, in this work, we focused on the influence of Al^{3+} on hIAPP (11-28) aggregration. By atomic force microscopy (AFM) and Thioflavin T (ThT) fluorescence spectroscopy, we found that Al^{3+} could dramatically inhibit fibril formation. Moreover, the X-ray photoelectron spectroscopy (XPS) data suggested that Al^{3+} could interact with hIAPP (11-28) fragment.

Materials and Methods

Materials

Human-IAPP (sequence KCNTATCATQRLANFLVHSSNNFGAIL SSTNVGSNTY) was purchased from AnaSpec Inc. (Fremont, USA). hIAPP (1-11), hIAPP (11-28), and hIAPP (28-37) peptide with the purity >98.35% were purchased from ChinaPeptides (Shanghai, China). $AlCl_3$, $ZnCl_2$, and ThT were purchased from Sigma-Aldrich (St Louis, USA). The Milli-Q water with a resistivity of 18.2 MΩ cm was used in all experiments.

Sample preparation

To prepare the fresh peptide solution, 1 mg of different peptide powder was first dissolved in 20 µl Milli-Q water (18.2 MΩ cm) as a stock solution and then stored at −20°C before use. To study the effect of metal ions on the aggregation of hIAPP peptides, $AlCl_3$, and $ZnCl_2$ were added respectively into peptide solution to a desired ion concentration (e.g. 100 and 200 µM) and a final fixed peptide concentration (20 µM). Then samples were incubated at 37°C for 3 days.

Atomic force microscopy

To prepare the samples for AFM imaging, 4~5 µl of incubated peptide solution was dropped on freshly cleaved mica surface. After drying in humidity control chamber at room temperature, the samples were ready for AFM image. AFM experiments were performed by using Nanoscope V Multimode 8 (Bruker, Karlsruhe, Germany) in tapping mode under ambient condition. The tips used were Mikromash NSC11 (NanoWorld AG, Schaffhausen, Switzerland) with resonance frequency of ~330 kHz and spring constant of ~40 N/m. AFM data were analyzed with NanoScope Analysis V1.20 software.

ThT fluorescence spectroscopy

To study the kinetics of fibril formation progress, ThT fluorescence measurement was performed using a Fluoroskan Ascent flurorescence spectrophotometer (Thermo Scientific, Waltham, USA). The fluorescence intensity was recorded every 5 min using 440 nm excitation and 484 nm emission filters. To prepare samples for fluorescence measurement, AlCl3 and $ZnCl_2$ with different concentrations (100 and 200 µM), 20 µM hIAPP (11-28) and 25 µM ThT were added in 96-well microtitre plate (Thermo Scientific Nunc, Waltham, USA). At least five set of measurements were carried out for each tested concentration of metal ions. And the final results were averaged.

Micro-Fourier Transform infrared spectroscopy

The secondary structures of peptides were also monitored at room temperature by an agilent cary660 spectrometer (Agilent, Santa Clara, USA). A drop of 2~3 µl incubated solution was spotted on the diamond surface and then dried with an infrared lamp. The absorbance spectra of different samples were collected with a resolution of 0.4 cm^{-1}. Fourier Transform infrared spectroscopy (FTIR) analysis of the data focused on the amide I mode, which is known to be a useful indicator of peptide secondary structures.

X-ray photoelectron spectroscopy

XPS measurement of different samples were carried out using an Axis Ultra DLD instrument (Kratos company, Manchester, UK) equipped with a monochromatic Al Ka (1486.7 eV photons). For XPS sample preparation, 20 µl incubated solution [20 µM hIAPP (11-28) with 200 µM $AlCl_3$] was deposited on a gold substrate and dried in a vacuum oven. All spectra were recorded in the constant pass energy mode of the analyzer using the monochromatic Al Ka X-ray source.

Results and Discussion

Figure 1A shows that 20 µM hIAPP (1-37) formed a various fibrillar structures after 3 days incubation alone at 37°C. While in the

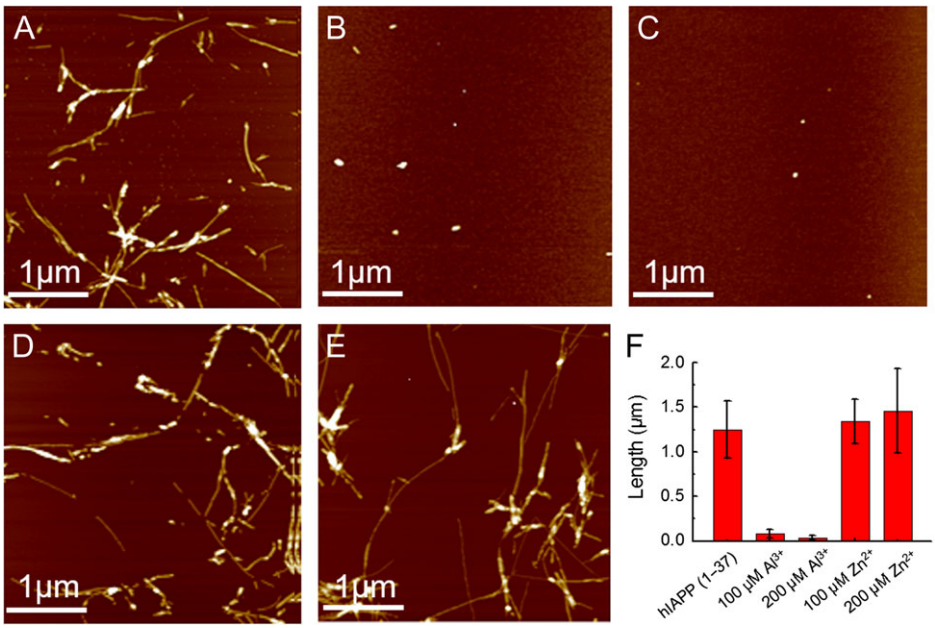

Figure 1. AFM images of hIAPP incubated at 37°C for 3 days in the presence or absence of metal ions (A) hIAPP incubated alone. (B) and (C) hIAPP incubated with 100 and 200 µM $AlCl_3$, respectively. (D) and (E) hIAPP incubated with 100 and 200 µM $ZnCl_2$, respectively. (F) The statistical diagram of lengths of hIAPP aggregation with or without metal ions.

presence of 100 μM Al^{3+}, the aggregation was strongly inhibited, only several granular structures were observed on the mica surface (**Fig. 1B,C**). By contrast, with the addition of 100 μM Zn^{2+}, peptide aggregation was accelerated slightly to form longer fibrillar structures (**Fig. 1D,E**), which is in agreement with the previous report [28]. **Figure 1F** illustrates the corresponding statistical diagram of fibril lengths formed at different condition, suggesting that Al^{3+} could remarkably prevent fibril formation, while Zn^{2+} has a modest impact on promoting the fibril growth. The aggregration of three hIAPP fragments, including hIAPP (1-11), hIAPP (11-28), and hIAPP (28-37) were also detected by AFM. It was found that only hIAPP (11-28) fragment formed fibrillar aggregates, while hIAPP (1-11) and hIAPP (28-37) appeared granular and spherical particles (**Fig. 2**). Therefore, we believe that hIAPP (11-28) fragment is the main region that contributes to the formation of β-sheet structures, which is consistent with a previous study [27]. In addition, the AFM images clearly revealed that, similar to hIAPP (1-37), Al^{3+} could also restrain hIAPP (11-28) fibrillation, only some monomers were observed in the image (**Fig. 3A–C**), while in the presence of Zn^{2+}, hIAPP (11-28) fibril formation was promoted (**Fig. 3D–F**).

Since $AlCl_3$ also changes the solution pH, we also checked the effect of the pH value on the fibrils formation. **Supplementary Figure S1** demonstrated that a change in the pH alone (in the absence of aluminum) to a value of that in the presence of aluminum did not cause any significant inhibition of amyloid formation.

It is well known that ThT could specifically bind with amyloid fibrils with cross-β-sheet structures, producing a new emission peak around 482 nm. Therefore, it has been widely used to study the kinetics of fibrils formation. Due to the importance of hIAPP (11-28) in fibrils formation, ThT fluorescence spectroscopy was performed to obtain the kinetic information of the effects of the Al ions on its fibrillization process of hIAPP (11-28). As shown in **Fig. 4**, for hIAPP (11-28) alone, the ThT fluorescence curve consists of an initial lag period, fast elongation phase and final plateau phase with maximal fluorescence intensity, which is comparable to the previous reported data [29]. However, in the presence of 200 μM Al^{3+}, almost no change in ThT fluorescence was observed. When the concentration of Al^{3+} was reduced to 100 μM, the ThT fluorescence intensity was slightly increased, indicating that the aggregation process of hIAPP (11-28) was seriously inhibited by Al^{3+}. By contrast,

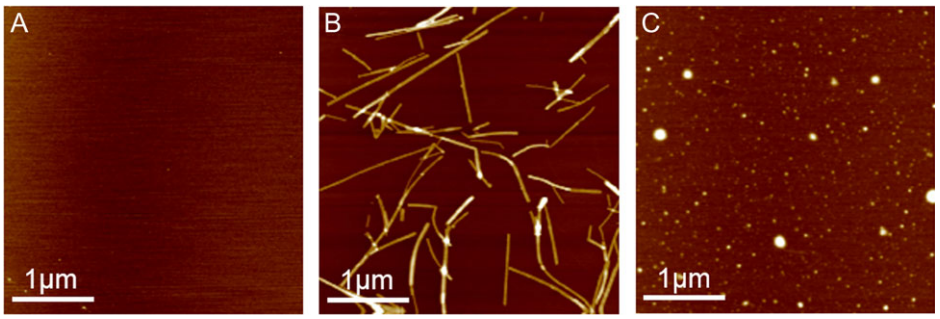

Figure 2. AFM images of three peptide fragments incubated at 37°C for 3 days (A) hIAPP (1-11), (B) hIAPP (11-28), and (C) hIAPP (28-37).

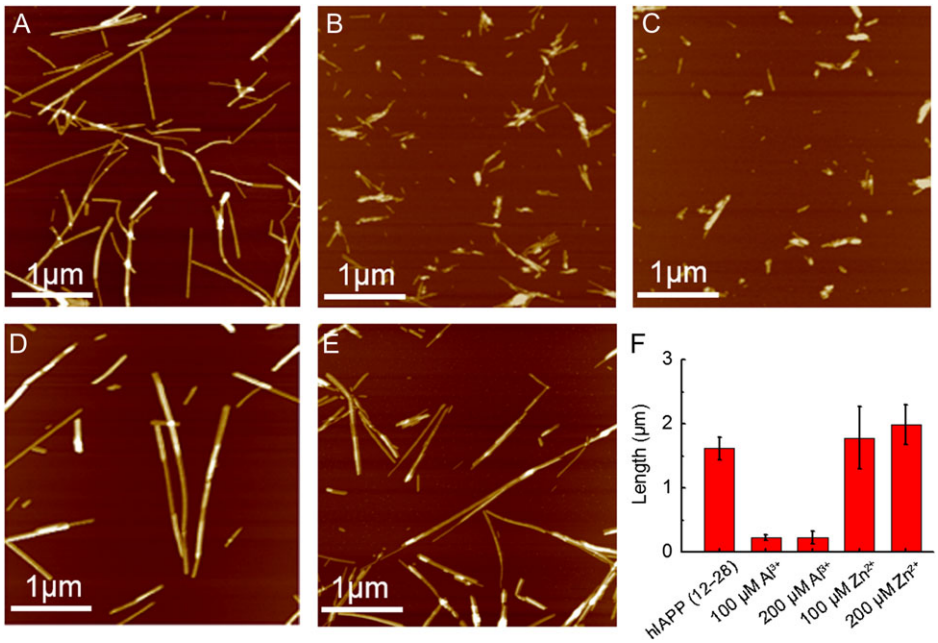

Figure 3. AFM images of hIAPP incubated with or without metal ions at 37°C for 3 days (A) hIAPP (11-28) incubated alone. (B) and (C) hIAPP (11-28) incubated with 100 and 200 μM $AlCl_3$, respectively. (D) and (E) hIAPP (11-28) incubated with 100 and 200 μM $ZnCl_2$, respectively. (F) The statistical diagram of lengths of hIAPP (11-28) aggregation with or without metal ions.

when hIAPP (11-28) was incubated with Zn^{2+} (100 and 200 μM), the ThT signal became somewhat stronger than hIAPP (11-28) incubated alone. Interestingly, although Zn^{2+} had a promoting effect on fibril aggregation to a certain degree, the initial lag time in the presence of Zn^{2+} was slightly delayed. It is probably because of the decreased nucleation rate caused by Zn^{2+}, this phenomenon was also observed by Brender *et al.* [30].

We also monitored the secondary structures of protein in the presence or absence of Al^{3+} using Micro-FTIR, a spectroscopy technique that provide information about the amide I and II bands. **Figure 5A** shows the representative Micro-FTIR spectra of hIAPP (11-28) with and without 3 days of incubation with Al^{3+} at 37°C. For hIAPP (11-28) alone, only one peak around 1630 cm^{-1} was observed, which is assigned to β-sheet structure [31]. In the presence of 100 μM Al^{3+}, a small shoulder peak around 1660 cm^{-1} appeared.

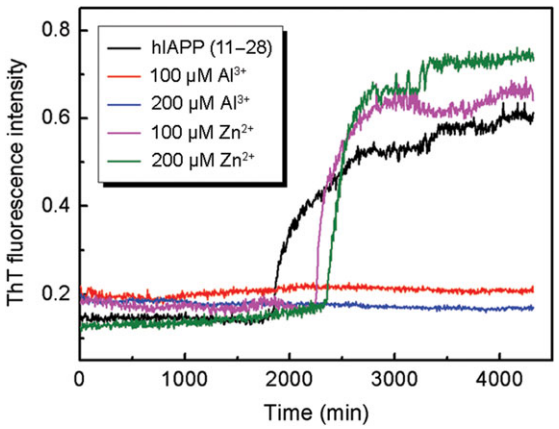

Figure 4. Kinetic analysis of hIAPP (11-28) fibril formation ThT fluorescence was measured in the absence (black) or the presence of 100 (red) and 200 μM (blue) of Al^{3+} or the presence of 100 (magenta) and 200 μM (olive) of Zn^{2+}.

This peak could be attributed to either random coil or helical structures [32]. It can be speculated that hIAPP (11-28) fibrils display the co-existence of β-sheet and α-helix structures in the presence of low concentration Al^{3+}. With the further increase of Al^{3+} concentration to 200 μM, the peak intensity at 1630 cm^{-1} decreased drastically, yielding predominant α-helix structures. However, the intensity of absorption peaks at 1630 cm^{-1} for hIAPP (11-28) incubated with Zn^{2+} was slightly increased compared with the hIAPP (11-28) incubated alone (**Fig. 5B**). These results indicated that hIAPP (11-28) aggregation was suppressed markedly by the presence of Al^{3+}, whereas in the presence of Zn^{2+} only very little difference could be observed. These results are also consistent with our AFM and ThT fluorescence results.

We further used XPS to explore the interaction between hIAPP (11-28) and Al^{3+}. XPS can be very sensitive to characterize the chemical form of atoms [33]. We observed one peak in XPS at around 119.4 eV when hIAPP (11-28) was co-incubated with Al^{3+} (**Fig. 6B**). For comparison, we also measured the specture of $AlCl_3$ (**Fig. 6A**). There are two peaks at around 118.3 and 109.5 eV which can be assigned to Al^{3+} and broad Au substrate respectively [25,34]. Importantly, when co-incubated with hIAPP (11-28), the peak of Al^{3+} at 119.4 eV was considerably larger than that at 118.4 eV in the spectrum from $AlCl_3$, suggesting that Al ions might form chemical bonds with neighboring atoms. This result agreed well with the theoretical calculation that Al ions could simultaneously bind to the amide nitrogen and carbonyl oxygen atoms of the peptide backbone [25]. Therefore, it could destroy the secondary structures of the protein and thus inhibit the formation of fibril structures.

In summary, we have investigated the effect of Al ions on hIAPP (11-28) peptide aggregation. Our results showed that Al^{3+} had strong inhibiting effects on the peptide self-assembly behavior. It could modulate the final fibrillar structure as well as aggregation kinetics. XPS data suggested that Al ions could interact with hIAPP (11-28) and might destroy the secondary structures of hIAPP (11-28). In several neurodegenerative diseases, especially AD, spherical aggregates are often found in tissue deposits. Therefore, Al ions may play

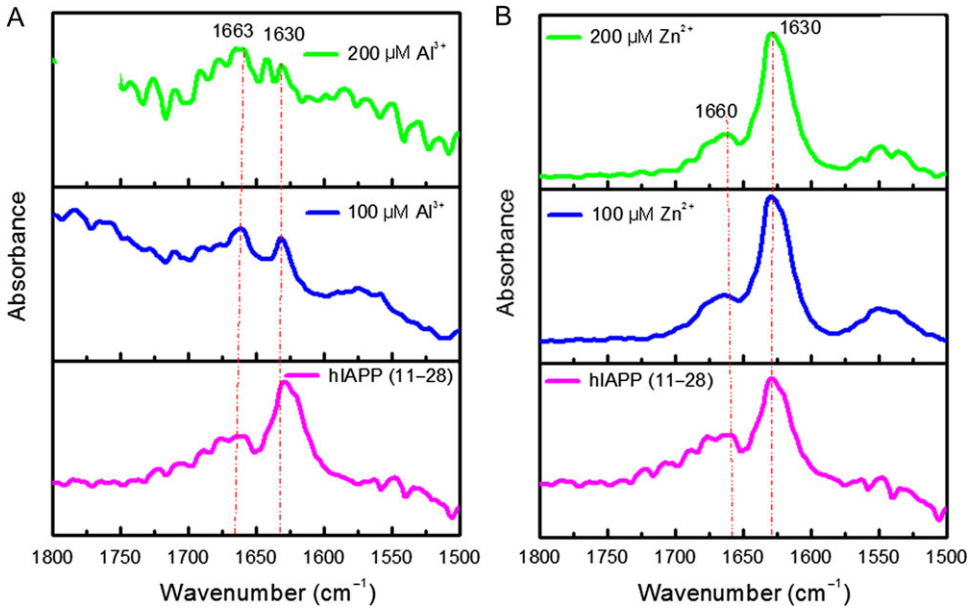

Figure 5. Micro-FTIR spectra of hIAPP (11-28) after incubation at 37°C for 3 days in the presence or absence of metal ions (A) hIAPP (11-28) with or without Al^{3+}. (B) hIAPP (11-28) with or without Zn^{2+}.

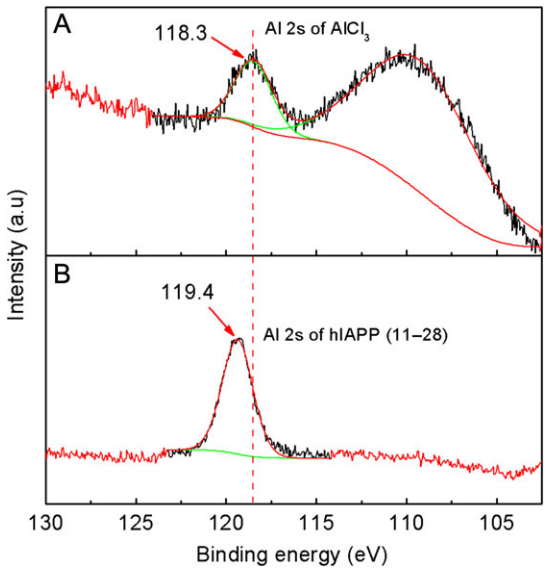

Figure 6. X-ray photoelectron spectra of aluminum chloride and hIAPP (11-28)
(A) aluminum chloride. (B) hIAPP (11-28) mixed with Al ions. The peak of Al^{3+} mixed with hIAPP (11-28) at 119.4 eV was considerably larger than that at 118.4 eV in the spectrum from $AlCl_3$, suggesting that Al ions might form chemical bonds with neighboring atoms.

an important role in fibrillar deposition *in vivo*. In contrast, Zn^{2+} could accelerate hIAPP (11-28) fibrillation in some way, we speculate that it may be caused by the fact that Zn^{2+} has a strong affinity for the imidaziole group of the histidine residue [30]. Our study may provide an insight into the role of metal ions in the aggregation of amyloid peptides.

Supplementary Data

Supplementary data is available at *Acta Biochimica et Biophysica Sinica* online.

Funding

This work was supported by the National Natural Science Foundation of China (Nos. 1147417, 11375253, and 31670871), the Natural Science Foundation of Zhejiang Province (No. LY14A040002), and the K. C. Wong Magna Fund in Ningbo University.

References

1. Dobson CM. Principles of protein folding, misfolding and aggregation. *Semin Cell Dev Biol* 2004, 15: 3–16.
2. Ashraf GM, Greig NH, Khan TA, Hassan I, Tabrez S, Shakil S, Sheikh IA, *et al*. Protein misfolding and aggregation in Alzheimer's disease and type 2 diabetes mellitus. *CNS Neurol Disord Drug Targets* 2014, 13: 1280–1293.
3. Detoma AS, Salamekh S, Ramamoorthy A, Lim MH. Misfolded proteins in Alzheimer's disease and type II diabetes. *Chem Soc Rev* 2012, 41: 608–621.
4. Kahn SE, Andrikopoulos S, Verchere CB. Islet amyloid: a long-recognized but underappreciated pathological feature of type 2 diabetes. *Diabetes* 1999, 48: 241–253.
5. Association AD. Diagnosis and classification of diabetes mellitus. *Diabetes Care* 2010, 33: s62–s69.
6. Hayden MR, Tyagi SC, Kerklo MM, Nicolls MR. Type 2 diabetes mellitus as a conformational disease. *J* Pancreas 2005, 6: 287–302.
7. Westermark P, Andersson A, Westermark GT. Islet amyloid polypeptide, islet amyloid, and diabetes mellitus. *Physiol Rev* 2011, 91: 795–826.
8. Schmitz O, Brock B, Rungby J. Amylin agonists: a novel approach in the treatment of diabetes. *Diabetes* 2004, 53: S233–S238.
9. Konarkowska B, Aitken JF, Kistler J, Zhang S, Cooper GJ. The aggregation potential of human amylin determines its cytotoxicity towards islet β-cells. *FEBS J* 2006, 273: 3614–3624.
10. Cooper GJ, Willis AC, Clark A, Turner RC, Sim RB, Reid KBM. Purification and characterization of a peptide from amyloid-rich pancreases of type 2 diabetic patients. *Proc Natl Acad Sci USA* 1987, 84: 8628–8632.
11. Zraika S, Hull RL, Udayasankar J, Aston-Mourney K, Subramanian SL, Kisilevsky R, Szarek WA, *et al*. Oxidative stress is induced by islet amyloid formation and time-dependently mediates amyloid-induced beta cell apoptosis. *Diabetologia* 2009, 52: 626–635.
12. Höppener JW, Ahrén B, Lips CJ. Islet amyloid and type 2 diabetes mellitus. *New Engl J Med* 2000, 343: 411–419.
13. Wong AG, Wu C, Hannaberry E, Watson MD, Shea JE, Raleigh DP. Analysis of the amyloidogenic potential of pufferfish (Takifugu rubripes) islet amyloid polypeptide highlights the limitations of thioflavin-T assays and the difficulties in defining amyloidogenicity. *Biochemistry* 2016, 55: 510–518.
14. Wang W, Nema S, Teagarden D. Protein aggregation—pathways and influencing factors. *Int J Pharm* 2010, 390: 89–99.
15. Malisauskas M, Zamotin V, Jass J, Noppe W, Dobson CM, Morozovaroche LA. Amyloid protofilaments from the calcium-binding protein equine lysozyme: formation of ring and linear structures depends on pH and metal ion concentration. *J Mol Biol* 2003, 330: 879–890.
16. Gursky O, Aleshkov S. Temperature-dependent beta-sheet formation in beta-amyloid Abeta 1–40 peptide in water: uncoupling L-structure folding from aggregation. *Biochim Biophys Acta* 2000, 1476: 93–102.
17. Faller P, Hureau C, Berthoumieu O. Role of metal ions in the self-assembly of the Alzheimer's amyloid-β peptide. *Inorg Chem* 2013, 52: 12193–12206.
18. Pramanik D, Ghosh C, Dey SG. Heme-Cu bound Aβ peptides: spectroscopic characterization, reactivity, and relevance to Alzheimer's disease. *J Am Chem Soc* 2011, 133: 15545–15552.
19. Ha C, Ryu J, Park CB. Metal ions differentially influence the aggregation and deposition of Alzheimer's β-amyloid on a solid template. *Biochemistry* 2007, 46: 6118–6125.
20. Miller LM, Wang Q, Telivala TP, Smith RJ, Lanzirotti A, Miklossy J. Synchrotron-based infrared and X-ray imaging shows focalized accumulation of Cu and Zn co-localized with β-amyloid deposits in Alzheimer's disease. *J Struct Biol* 2006, 155: 30–37.
21. Lovell MA, Robertson JD, Teesdale WJ, Campbell JL, Markesbery WR. Copper, iron and zinc in Alzheimer's disease senile plaques. *J Neurol Sci* 1998, 158: 47–52.
22. Khan FA, Jameil N, Arjumand S, Khan FM, Tabassum H, Alenzi N, Hijazy S, *et al*. Comparative study of serum copper, iron, magnesium, and zinc in type 2 diabetes-associated proteinuria. *Biol Trace Elem Res* 2015, 168: 321–329.
23. Sinopoli A, Magrì A, Milardi D, Pappalardo M, Pucci P, Flagiello A, Titman JJ, *et al*. The role of copper(II) in the aggregation of human amylin. *Metallomics* 2014, 6: 1841–1852.
24. Suzuki K, Miura T, Takeuchi H. Inhibitory effect of copper(II) on zinc (II)-induced aggregation of amyloid β-peptide. *Biochem Biophys Res Commun* 2001, 285: 991–996.
25. Song B, Sun Q, Li H, Ge BS, Pan JS, Wee ATS, Zhang Y, *et al*. Irreversible denaturation of proteins through aluminum-induced formation of backbone ring structures. *Angew Chem Int Ed* 2014, 53: 6358–6363.
26. Janson J, Laedtke T, Parisi JE, O'Brien P, Petersen RC, Butler PC. Increased risk of type 2 diabetes in Alzheimer disease. *Diabetes* 2004, 53: 474–481.
27. Qi R, Luo Y, Ma B, Nussinov R, Wei G. Conformational distribution and α-helix to β-sheet transition of human amylin fragment dimmer. *Biomacromolecules* 2014, 15: 122–131.

28. Brender JR, Krishnamoorthy J, Messina GM, Deb A, Vivekanandan S, La Rosa C, Penner-Hahn JE, *et al*. Zinc stabilization of prefibrillar oligomers of human islet amyloid polypeptide. *Chem Commun* 2013, 49: 3339–3341.
29. Faller P, Hureau C, Berthoumieu O. Role of metal ions in the self-assembly of the Alzheimer's amyloid-β peptide. *Inorg Chem* 2013, 52: 12193–12206.
30. Brender JR, Hartman K, Nanga RPR, Popovych N, Bea RD, Vivekanandan S, Marsh ENG, *et al*. Role of zinc in human islet amyloid polypeptide aggregation. *J Am Chem Soc* 2010, 132: 8973–8983.
31. Goormaghtigh E, Cabiaux V, Ruysschaert JM. Determination of soluble and membrane protein structure by Fourier transform infrared spectroscopy. *Subcell Biochem* 994: 363–403.
32. Kong J, Yu S. Fourier transform infrared spectroscopic analysis of protein secondary structures. *Acta Biochim Biophys Sin* 2007, 39: 549–559.
33. Fadley CS. X-ray photoelectron spectroscopy: progress and perspectives. *J Electron Spectrosc* 2010, 178: 2–32.
34. Duong LV, Wood BJ, Kloprogge JT. XPS study of basic aluminum sulphate and basic aluminium nitrate. *Mater Lett* 2005, 59: 1932–1936.